Supporting Information to "Circum-Antarctic abundance and properties of CCN and INP"

Christian Tatzelt[1], Silvia Henning[1], André Welti[2], Andrea Baccarini[3,4], Markus Hartmann[1], Martin Gysel-Beer[3], Manuela van Pinxteren[1], Robin L. Modini[3], Julia Schmale[3,4], and Frank Stratmann[1]

[1]Leibniz Institute for Tropospheric Research, Permoserstrasse 15, 04318 Leipzig, Germany
[2]Finnish Meteorological Institute, Erik Palménin aukio 1, FI-00560 Helsinki, Finland
[3]Laboratory of Atmospheric Chemistry, Paul Scherrer Institute, 5232 Villigen PSI, Switzerland
[4]Extreme Environments Research Laboratory, École Polytechnique Fédérale de Lausanne, School of Architecture, Civil and Environmental Engineering, Lausanne, Switzerland

Correspondence: Silvia Henning (silvia.henning@tropos.de), Julia Schmale (julia.schmale@epfl.ch)

Contents

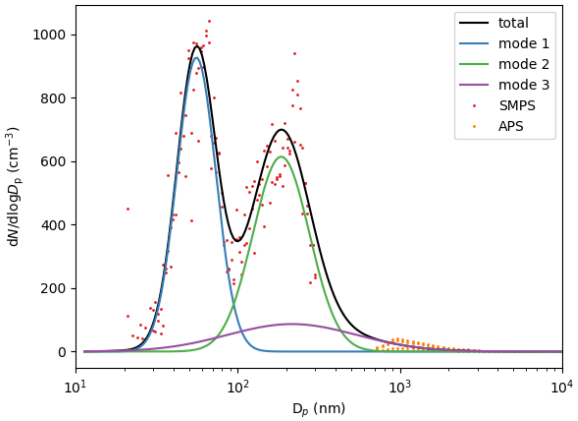

Figure S1. An example for the results of the mode-fitting approach applied to the output of the SMPS and APS instruments. PNSD from the SMPS (red) and APS instruments (orange) are given as dots. The three fitted log-normal distributions (Aitken mode, blue; accumulation mode, green; sea spray mode, lila) and the sum of the three modes (total PNSD, black) are given as lines.

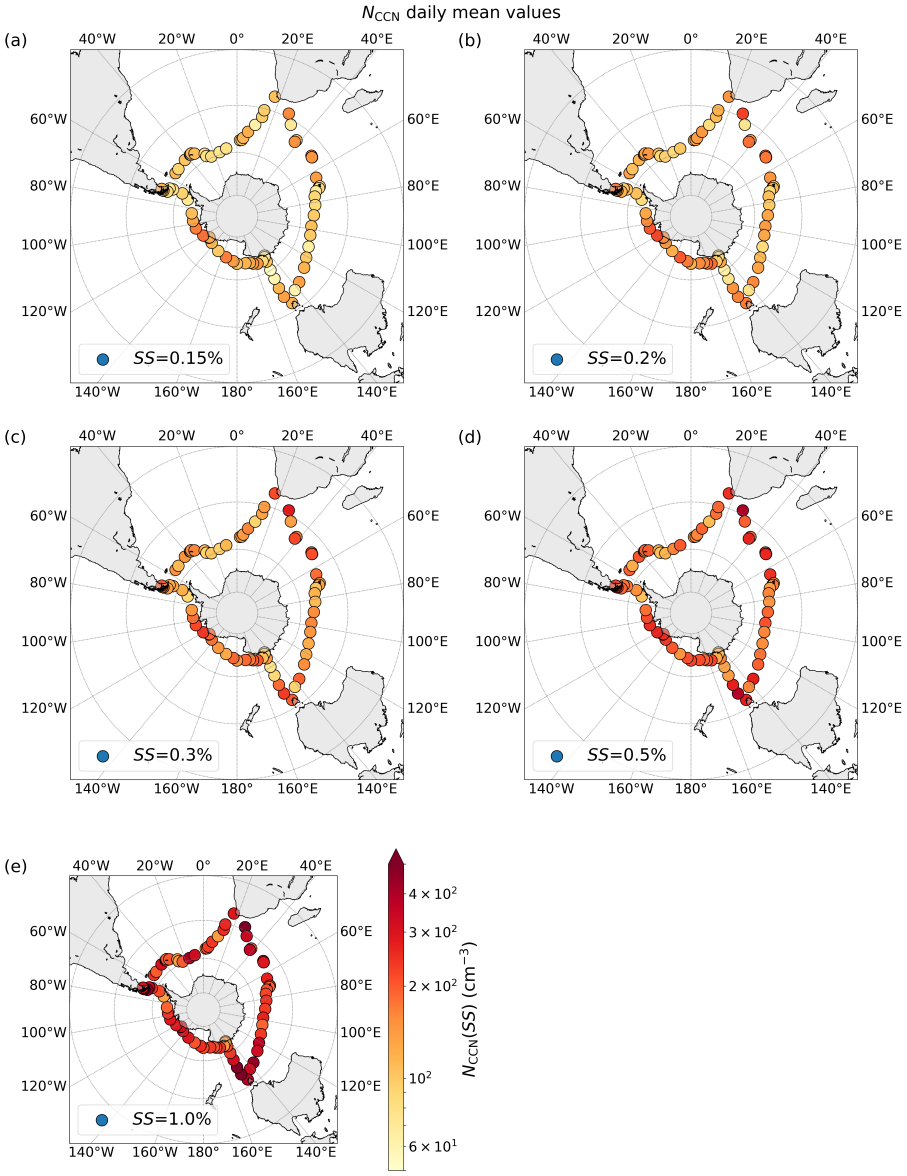

Figure S2. Average daily values of CCN number concentration (N_{CCN}) at a supersaturation (SS) of 0.15 (a), 0.2 (b), 0.3 (c), 0.5 (d), and 1% (e) throughout the cruise, given at the midpoint of the respective cruise track of that day.

Table S1. Overview of the CCN number concentration (N_{CCN}) and critical dry diameter (D_{crit}) values at a given level of supersaturation (SS) throughout and for parts of the cruise, given as geometric mean value (and a factor of respective one geometric standard deviation). Additionally, the averages of the total particle concentration (N_{total}) and the aerosol particle hygroscopicity parameter (κ) at given SS presented as median values and respective inter-quartile range.

	Legs 1–3	Leg 1	Leg 2	Leg 3
N_{total} (cm^{-3})	305.04 (225.77, 451.84)	389.75 (272.06, 539.29)	277.00 (211.34, 382.17)	318.76 (235.02, 442.93)
$N_{\mathrm{CCN}}(SS)$ (cm^{-3})				
$SS = 0.15\%$	88.64 (53.28, 147.48)	90.49 (52.04, 157.33)	94.20 (59.19, 149.92)	78.61 (47.29, 130.69)
$SS = 0.2\%$	111.79 (67.98, 183.82)	113.56 (67.28, 191.67)	119.48 (76.03, 187.76)	98.63 (58.85, 165.29)
$SS = 0.3\%$	132.52 (79.41, 221.16)	133.83 (80.84, 221.54)	143.39 (88.97, 231.11)	115.50 (66.95, 199.27)
$SS = 0.5\%$	171.69 (101.49, 290.47)	172.18 (106.83, 277.51)	185.44 (111.84, 307.47)	150.71 (84.43, 269.05)
$SS = 1\%$	247.98 (145.28, 423.28)	241.12 (157.20, 369.82)	257.79 (146.73, 452.92)	239.56 (133.96, 428.39)
$D_{\mathrm{crit}}(SS)$ (nm)				
$SS = 0.15\%$	109.40 (100.29, 119.34)	112.56 (101.94, 124.29)	108.61 (99.91, 118.07)	110.05 (100.98, 119.94)
$SS = 0.2\%$	84.07 (72.77, 97.12)	89.86 (75.98, 106.28)	81.78 (71.46, 93.59)	86.52 (75.97, 98.54)
$SS = 0.3\%$	66.23 (56.37, 77.83)	72.77 (60.36, 87.72)	64.15 (55.43, 74.24)	66.73 (57.51, 77.42)
$SS = 0.5\%$	47.04 (39.98, 55.34)	52.23 (42.01, 63.42)	45.58 (39.42, 52.69)	47.18 (40.84, 54.52)
$SS = 1\%$	30.22 (25.73, 35.48)	32.90 (27.73, 39.04)	29.46 (25.20, 34.44)	30.22 (26.18, 34.88)
$\kappa(SS)$				
$SS = 0.15\%$	0.50 (0.40, 0.60)	0.42 (0.33, 0.53)	0.51 (0.42, 0.61)	0.48 (0.40, 0.59)
$SS = 0.2\%$	0.61 (0.44, 0.82)	0.43 (0.30, 0.66)	0.67 (0.50, 0.89)	0.54 (0.42, 0.72)
$SS = 0.3\%$	0.57 (0.39, 0.78)	0.36 (0.24, 0.60)	0.63 (0.46, 0.84)	0.55 (0.41, 0.73)
$SS = 0.5\%$	0.55 (0.39, 0.79)	0.34 (0.23, 0.58)	0.60 (0.45, 0.84)	0.54 (0.40, 0.74)
$SS = 1\%$	0.52 (0.38, 0.70)	0.39 (0.24, 0.54)	0.55 (0.42, 0.76)	0.52 (0.38, 0.68)

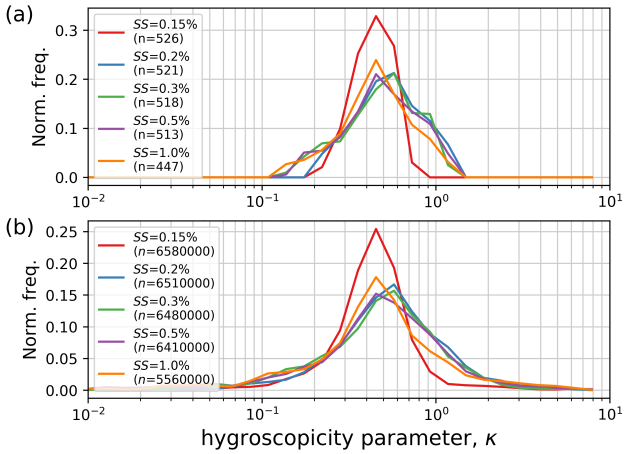

Figure S3. Normalized probability density function of hygroscopicity parameter κ for levels of supersaturation 0.15, 0.2, 0.3, 0.5, 1% (colour-coded) for legs 1-3 without (a) performing MCS to assess the measurement uncertainty and (b) without the exclusion of κ values that resulted from D_{crit} outside of 10^{th} to 90^{th} percentile range (per SS). The number of data points is indicated (n).

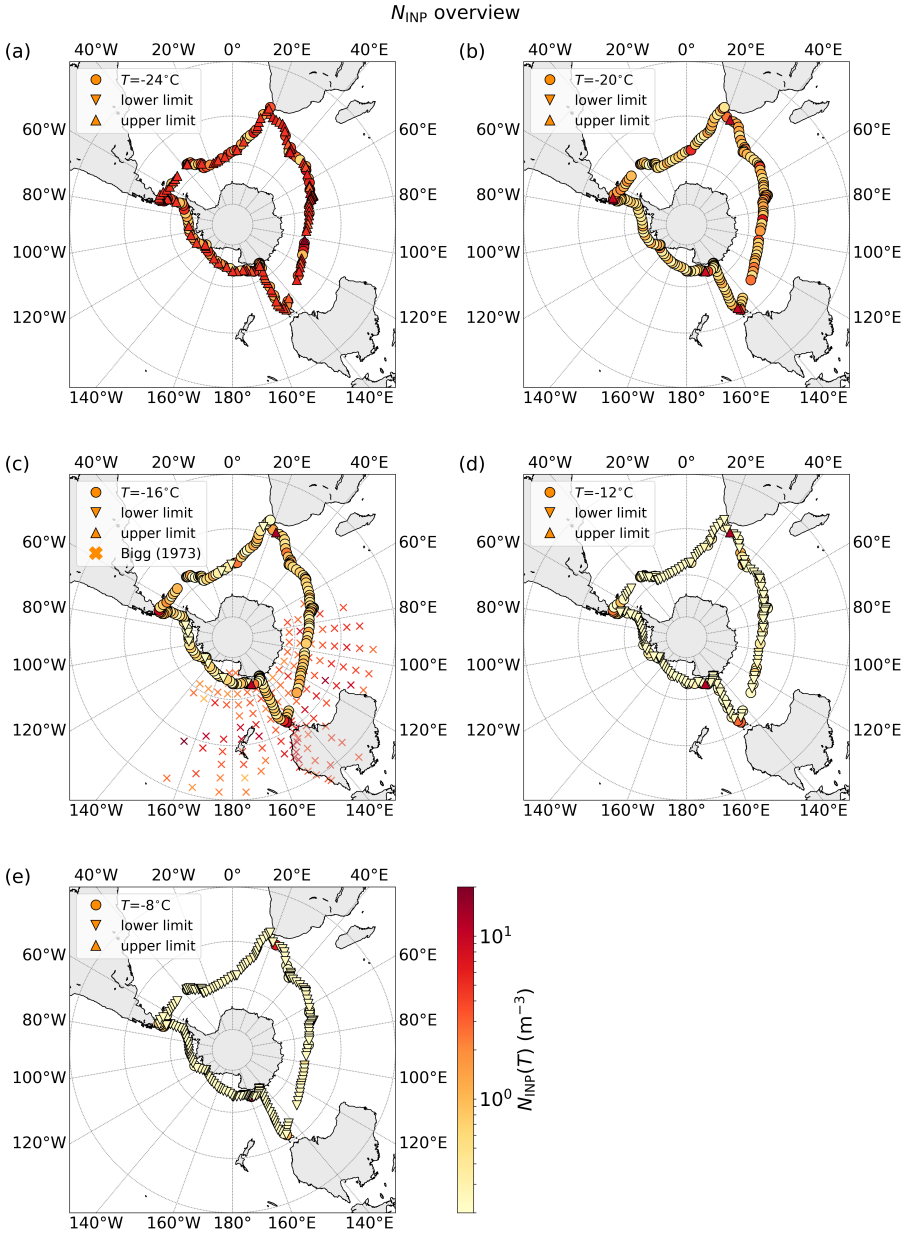

Figure S4. INP concentration at (a) -8, (b) -12, (c) -16, (d) -20, and (e) -24°C from 8 h sampled LV filters (circles). Filters at lower (upper) end of detectable range are indicated as downward (upward) triangles. Values of $N_{\mathrm{INP},-15}$ from Bigg (1973) are provided in (c) for comparison (crosses). A correction of the $N_{\mathrm{INP},-15}$ values from Bigg (1973) was applied, following the the supporting information to McCluskey et al. (2018).

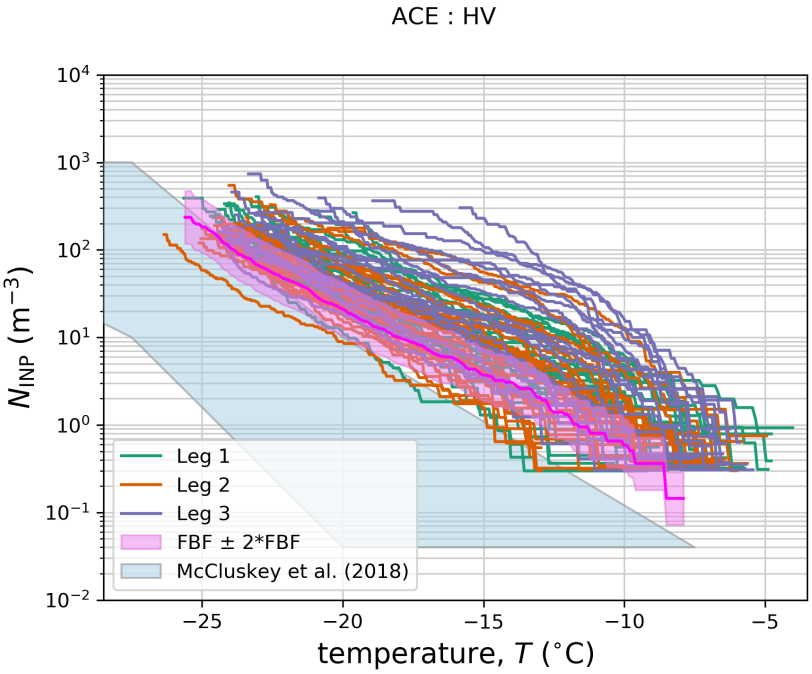

Figure S5. INP concentration as function of temperature for HV filters sampled for 24 h. Average spectra of field blank filters (FBF) and corresponding factor two (pink line and area), and data range from McCluskey et al. (2018) (light blue) are given for reference.

Table S2. Overview of the LV sampling INP concentrations ($N_{\mathrm{INP,LV}}$) encountered throughout and during parts of the cruise, given as mean, median and geometric mean (and a factor of respective one geometric standard deviation) values. The number of considered samples is indicated (n). Additionally, averaging was performed with the inclusion of values on the detectable range and values are given under N^{*}_{INP}.

	mean	median	gmean (gSD)	n
$N_{\mathrm{INP,LV}}(T)$ (m^{-3})				
$T = -24^{\circ}\mathrm{C}$	66.95	64.78	61.45 (40.07, 94.25)	105
$T = -20^{\circ}\mathrm{C}$	13.87	8.57	9.43 (4.21, 21.15)	237
$T = -16^{\circ}\mathrm{C}$	4.41	1.18	1.44 (0.41, 5.10)	237
$T = -12^{\circ}\mathrm{C}$	2.66	0.42	0.72 (0.17, 2.99)	120
$T = -8^{\circ}\mathrm{C}$	1.67	0.46	0.58 (0.18, 1.84)	46
$N^{\star}_{\mathrm{INP,LV}}(T)$ (m^{-3})				
$T = -24^{\circ}\mathrm{C}$	85.22	97.65	80.39 (55.48, 116.48)	252
$T = -20^{\circ}\mathrm{C}$	18.75	8.84	10.82 (4.16, 28.15)	252
$T = -16^{\circ}\mathrm{C}$	6.11	1.17	1.46 (0.35, 5.97)	252
$T = -12^{\circ}\mathrm{C}$	2.15	0.23	0.41 (0.12, 1.43)	252
$T = -8^{\circ}\mathrm{C}$	0.49	0.23	0.27 (0.14, 0.50)	252

Table S3. Mean INP concentration of LV sampling field blank filters ($N_{\mathrm{INP,FBF}}$) at selected temperatures (T).

T	$N_{\mathrm{INP,LV,FBF}}$ (m^{-3})
$-24°\mathrm{C}$	57.76
$-20°\mathrm{C}$	7.72
$-16°\mathrm{C}$	0.59
$-12°\mathrm{C}$	0.08
$-8°\mathrm{C}$	-

Table S4. Overview of the HV sampling INP concentrations ($N_{\mathrm{INP,HV}}$) encountered throughout and during parts of the cruise, given as mean, median and geometric mean (and a factor of respective one geometric standard deviation) values. Averaging was performed with the inclusion of values on the detectable range and the number of considered samples is indicated (n).

	mean	median	gmean (gSD)	n
$N_{\mathrm{INP,HV}}(T)$ (m^{-3})				
$T = -24^{\circ}\mathrm{C}$	206.08	176.07	185.52 (118.70, 289.94)	79
$T = -20^{\circ}\mathrm{C}$	70.28	40.63	48.52 (21.51, 109.45)	79
$T = -16^{\circ}\mathrm{C}$	25.03	12.81	13.39 (4.77, 37.60)	79
$T = -12^{\circ}\mathrm{C}$	6.82	3.10	3.17 (0.90, 11.15)	79
$T = -8^{\circ}\mathrm{C}$	0.94	0.54	0.69 (0.34, 1.43)	79

Table S5. Overview of PM_{10}, sodium and methanesulfonic acid (MSA) mass concentrations throughout the cruise, given as median values (and inter-quartile range).

N (µg m^{-3})	Legs 1–3	Leg 1	Leg 2	Leg 3
PM_{10}	32.35 (26.05, 49.60)	42.40 (27.30, 52.60)	31.05 (23.48, 47.48)	33.30 (26.20, 50.70)
sodium	2.75 (1.81, 3.89)	3.55 (2.56, 4.92)	1.81 (0.97, 3.15)	2.75 (2.24, 4.10)
MSA	0.10 (0.07, 0.14)	0.11 (0.08, 0.18)	0.11 (0.07, 0.21)	0.09 (0.06, 0.10)

References

Bigg, E.: Ice nucleus concentrations in remote areas, Journal of the Atmospheric Sciences, 30, 1153–1157, https://doi.org/10.1175/1520-0469(1973)030<1153:INCIRA>2.0.CO;2, 1973.

McCluskey, C., Hill, T., Humphries, R., Rauker, A., Moreau, S., Strutton, P., Chambers, S., Williams, A., McRobert, I., Ward, J., et al.: Observations of ice nucleating particles over Southern Ocean waters, Geophysical Research Letters, 45, 11–989, https://doi.org/10.1029/2018GL079981, 2018.